J. Am. Soc. Mass Spectrom. (2019) 30:403–418
DOI: 10.1007/s13361-018-2089-5

RESEARCH ARTICLE

Various Multicharged Anions of Ginsenosides in Negative Electrospray Ionization with QTOF High-Resolution Mass Spectrometry

Nan Zhao,[1,2] Mengchun Cheng,[1] Shuai Huang,[1] Dan Liu,[1] Qiang Zhao,[1,3] Yunpeng Bai,[1] Xiaozhe Zhang[1]

[1]CAS Key Laboratory of Separation Sciences for Analytical Chemistry, Dalian Institute of Chemical Physics, Chinese Academy of Sciences, Zhongshan Road 457, 116023, Dalian, People's Republic of China
[2]University of Chinese Academy of Sciences, Yuquan Road 19, 100049, Beijing, People's Republic of China
[3]Key Laboratory of Structure-Based Drug Design & Discovery of Ministry of Education, Shenyang Pharmaceutical University, Shenyang, People's Republic of China

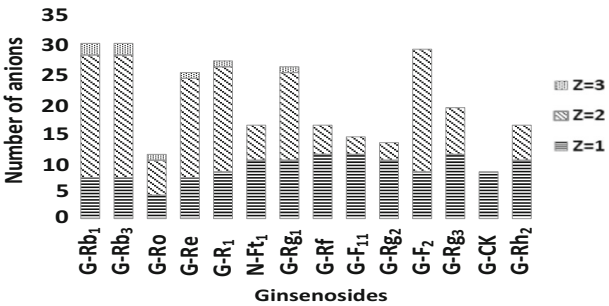

Abstract. When characterizing components from ginseng, we found a vast number of multicharged anions presented in the liquid chromatography–mass spectrometry (LC-MS) chromatograms. The source of these anions is unclear yet, while ginsenosides, the major components of ginseng, are the main suspected type of molecules because of their sugar moiety. Our investigation using 14 pure ginsenosides affirmed that the multicharged anions were formed by ginsenosides rather than other types of ingredients in ginseng. Various anions could be observed for each ginsenoside. These anions contain ions ($[M-2H]^{2-}$, $[M+Adduct]^{2-}$), as well as those formed by polymerization of at least two ginsenosides, such as $[nM-2H]^{2-}$, $[nM-H+Adduct]^{2-}$, and $[nM-3H]^{3-}$. The presence of so different types of ions from a ginsenoside explains the reason for the large number of anions in the LC-MS analysis of ginseng. We further found that formation of $[nM-2H]^{2-}$ ions was influenced by the number of sugar chains: ginsenosides containing two sugar chains produced all $[nM-2H]^{2-}$ ion types, whereas ginsenosides containing one sugar chain did not produce $[2M-2H]^{2-}$. Thus, $[2M-2H]^{2-}$ and $[3M-2H]^{2-}$ can be utilized to rapidly identify monodesmosidic and/or bidesmosidic ginsenosides as joint diagnostic anions. The position of the glycosyl radical might be the key factor affecting the formation of multicharged multimer ions from monodesmosidic ginsenosides. Consequently, three groups of ginsenoside isomers were differentiated by characteristic $[nM-2H]^{2-}$ anions. Using concentration-dependent characteristics and collision-induced dissociation (CID), we confirmed that $[nM-2H]^{2-}$ ions are non-covalently bound multimers whose aggregation has marked distinction between monodesmosidic and bidesmosidic ginsenosides, accounting for the differentiated formation of $[nM-2H]^{2-}$ between them.

Keywords: Electrospray ionization, Ginsenoside, Multicharged anion, Multimer, High-resolution mass spectrometry

Received: 9 April 2018/Revised: 6 October 2018/Accepted: 10 October 2018/Published Online: 14 January 2019

Introduction

Ginsenosides, also called ginseng saponins, are the major bioactive ingredients of the genus *Panax,* including *Panax ginseng* C. A. Meyer (PG, Asian or Korean ginseng),

Electronic supplementary material The online version of this article (https://doi.org/10.1007/s13361-018-2089-5) contains supplementary material, which is available to authorized users.

Correspondence to: Xiaozhe Zhang; *e-mail:* zhangxz@dicp.ac.cn

Panax quinquefolius L. (PQ, North American ginseng), and *Panax notoginseng* (Burkill) F.H. Chen (PN, Sanchi ginseng), which are widely used as medicinal herbs [1, 2]. Numerous studies have confirmed that compounds in this family exhibit a variety of pharmacological activities, including anti-aging [3, 4], anti-cancer [5, 6], anti-fatigue [7], anti-inflammatory [8, 9], memory enhancement [10], immunomodulatory [11], and neuroprotective effects [12]. To date, about 70 ginsenosides with diverse sapogenins have been isolated [13], and more than 640 ginsenosides have been identified or tentatively characterized from ginseng [14]. Moreover, the ginseng root contains 2–3% ginsenosides and Rb_1, Rb_2, Rc, Rd, Re, and Rg_1 account for more than 90% of total ginsenosides [15]. Ginsenosides are a class of natural product steroid glycosides and triterpene saponins. They are divided into dammarane, oleanane, and occotillol types on the basis of the carbon skeletons of their aglycones. Most known ginsenosides are classified as members of the dammarane family, which can be subdivided further into two groups, the protopanaxadiol (PPD) and protopanaxatriol (PPT) types. The PPD-type ginsenosides possess sugar moieties at the C-3 and/or C-20 positions, whereas the PPT-type ginsenosides have sugar moieties at the C-6 and/or C-20 sites. Furthermore, based on the attachment positions of the sugar chains, ginsenosides can be grouped into two categories: monodesmosidic and bidesmosidic ginsenosides, with glycosyl groups attached to the aglycones at one or two positions, respectively [16]. The chemical structures of the compounds determine their biological activities and minor structural differences can have a significant effect on their function. Remarkably, numerous isomers of ginsenosides exist because of the various types and diverse sites of sugar moieties. These may have different pharmacological activities and/or be present in different herbs of the *Panax* species. Therefore, structural analysis of ginsenosides and identification of isomerous ginsenosides are crucial for elucidating the structure-activity relationship of these saponins and allow for metabolite profiling of ginseng and other relevant research.

Quadrupole time-of-flight mass spectrometry (QTOF-MS), a typical high-resolution mass spectrometry (HRMS), provides several advantages in structural analysis, such as higher resolution and accuracy in mass measurements, and has become a powerful tool for the characterization and determination of ginsenosides [17, 18]. Electrospray ionization (ESI) is capable of ionizing ginsenosides for mass spectrometry analysis without complicated derivatization. Moreover, ESI-MS can be coupled with high-performance liquid chromatography (HPLC)/ultra-high-performance liquid chromatography (UPLC) to effectively separate ginsenosides and their isomers and improve the ionization efficiency for each ginsenoside. Furthermore, accurate molecular weight information of quasi-molecular ions can be obtained by high-resolution mass spectrometry (TOF analyzer) [19–21]. ESI coupled with tandem mass spectrometry (ESI-MS/MS) analysis allows for the characterization and elucidation of ginsenosides by collision-induced dissociation (CID), which is a mass spectrometry technique to induce fragmentation of molecular ions in the gas phase. Diagnostic product ions are produced by CID of the deprotonated precursor ions to obtain accurate structural information about ginsenosides. This information provides abundant and reliable data for the study of ginsenoside chemistry and metabolomics [22].

Both positive and negative ion modes have been employed for mass spectrometry analysis of ginsenosides in previous studies [16, 23, 24]. Ginsenosides are charged through protonation and/or cationization to form $[M+H]^+$ and $[M+Adduct]^+$ such as $[M+Na]^+$ and $[M+K]^+$, with the intensity of $[M+H]^+$ being much less than that of cationic adducts in general. A hetero atom with a lone pair of electrons in each outer layer of the molecule may combine with a proton to form a molecular ion $[M+H]^+$. In the positive ion mode, a compound can be ionized theoretically if it contains sites that will bind to proton, sodium, potassium, and/or other cations. Most organic compounds containing O and N meet these ionization requirements in the positive mode detection; hence, the selectivity becomes relatively poor, especially with complex substrates. In recent years, the negative mode ESI-MS has been applied increasingly to the analysis of ginsenosides. Under normal circumstances, $[M-H]^-$ of neutral ginsenosides are not easily obtained in the negative ion mode because a suitable deprotonation site is lacking. Since ginsenosides (like oligosaccharides) possess saccharide groups, they can be charged through the formation of adducts with various anions such as $[M+F]^-$, $[M+Cl]^-$, $[M+Br]^-$, $[M+HCOO]^-$, and $[M+AcO]^-$ to enhance their intensity for negative ESI-MS detection [25–27]. Moreover, compared to the positive ion mode, the negative ion mode has reduced background noise and higher selectivity. The analysis of ginsenosides in the negative ion mode has significant advantages over that of positive spectrum detection, especially in complex systems.

In our systematic characterization of constituents from ginseng, a large number of doubly and triply charged anions were observed in the negative ion ESI-MS spectra of ginseng extracts. Notably, these multicharged anions co-eluted with ginsenosides, with *m/z* values that were generally greater than the molecular weight of ginsenosides (M) and had certain numerical relationships between them. To our knowledge, doubly charged ions such as $[M-2H]^{2-}$, $[M-H+AcO]^{2-}$, and $[M+2AcO]^{2-}$ have been reported in the previous studies of mass spectrometry analysis of ginsenosides [16, 23], but their *m/z* values were obviously less than (approximately half) that of ginsenosides (singly charged ions $[M-H]^-$). Our calculations show that these multicharged anions are new ionic types of ginsenosides including doubly charged multimer anions $[nM-2H]^{2-}$ and $[nM-H+Adduct]^{2-}$ and triply charged anions $[nM-3H]^{3-}$, which have not been reported previously. In addition, structural relationships between multicharged anions and molecular structures of ginsenosides may exist. In this study, various species of ginsenoside reference substances were employed to investigate the mass spectral behavior of ginsenosides, expound the formation of multicharged ginsenosides anions, and determine the relationship between anions and molecular structures of ginsenosides, in order to

provide new methods for the rapid identification of the structure type of ginsenosides, especially ginsenoside isomers.

Experimental

Materials and Reagents

Fourteen ginsenoside reference standards, ginsenoside Rb_1, Rb_3, Re, Rf, Rg_1, Rg_2, Rg_3, Rh_2, Ro, F_2, compound K, notoginsenoside Ft_1, R_1, and pseudoginsenoside F_{11}, were purchased form Aladdin company (Shanghai, China). Ginseng reference material was obtained from the China National Institute for the Control of Pharmaceutical and Biological Products (Beijing, China). HPLC grade methanol and acetonitrile were obtained from Merck (Darmstadt, Germany). Formic acid for mass spectrometry was purchased from Sigma-Aldrich (MO, USA). The ultrapure deionized water was supplied by a Millipore Milli-Q water system (Milford, MA, USA).

Sample Preparation

Stock solutions of the 14 pure ginsenosides (ginsenoside Rb_1 1.80 mM, Rb_3 1.85 mM, Re 2.11 mM, Rf 2.50 mM, Rg_1 2.50 mM, Rg_2 2.55 mM, Rg_3 2.55 mM, Rh_2 3.21 mM, Ro 2.09 mM, F_2 2.55 mM, compound K 3.21 mM, notoginsenoside Ft_1 2.18 mM, R_1 2.14 mM, and pseudoginsenoside F_{11} 2.50 mM) were prepared individually in methanol. A mixture containing 14 reference standards was prepared by equal volume mixing of every stock solution. Working solutions were prepared by serial dilution of methanol to the desired final concentrations.

An easy-to-implement ultrasonic extraction method was employed for ginseng extraction. Briefly, 100 mg fine powder of ginseng reference material was weighed in a 2-mL microcentrifuge tube (EP tube) and treated with 0.5 mL of 50% methanol aqueous solution. The sample was vigorously mixed by a vortex mixer. Subsequently, the tube was placed in an ultrasonic cleaner (1130 W, 37 kHz) for 15 min. After being centrifuged at 12,000 rpm for 10 min, the supernatant was transferred into a new 2-mL EP tube while the extraction method was repeated with the residue. The pooled supernatants were filtered through a 0.22-μm filter and stored at 4 °C until analysis.

LC-MS/MS

Analysis was performed on an Agilent 1290 series ultra-high-performance liquid chromatograph (Agilent Technologies, Waldbron, Germany). An Agilent ZORBAX Eclipse Plus C18 (2.1 × 50 mm, 2.7 μm) was used for sample separation at 60 °C with a flow rate of 0.4 mL/min using 0.1% formic acid aqueous solution (A) and acetonitrile (B) as the mobile phase. The gradient elution program was 5–100% B at 0–10 min. The sample injection volume was 5 μL.

High-resolution MS and MS/MS analyses were performed on an Agilent 6520 QTOF mass spectrometer (Agilent Technologies, Santa Clara, CA, USA) via a dual ESI interface. For mass detection, the instrument was operated in the negative electrospray ion mode with the mass range *m/z* 50–3000. The operating parameters were optimized as follows: temperature of the drying gas 350 °C, drying gas (N_2) flow rate 8 L/min, pressure of the nebulizing gas 40 psi, capillary voltage 3500 V, fragmentor voltage 175 V, and skimmer voltage 65 V. CID was employed to study the fragmentation behavior of ginsenosides. In the CID mode, the collision energy was set from 5 to 80 V. Data recording and processing were performed with a Masshunter workstation (Agilent Technologies, Santa Clara, CA, USA).

Results and Discussion

Discovery of Various Multiply-Charged Anions Co-eluting with Ginsenosides in Ginseng Extract by UPLC-ESI-HRMS

In our unpublished research on identification of components from ginseng, a universal liquid chromatography–mass spectrometry (LC-MS) method was used to characterize diverse components. Most methods such as sample extraction solvent, mobile phase, and mass spectrometry parameters were quite conventional. The significant difference compared with previous studies was that we expanded the mass scan range to 3000 Da. Interestingly, we found a large number of multiply-charged anions co-eluting with ginsenosides during UPLC-ESI-HRMS analysis of ginseng extract. As shown in Figure 1a, many ginsenosides eluted between 3.5 and 5 min. Peaks I (t_R = 4.08 min) and II (t_R = 4.58 min) were selected to study multicharged ions co-eluting with ginsenosides. Based on accurate mass-to-charge ratio data, relevant adduct anions, and previous studies, a compound was tentatively identified as ginsenoside-A (GA) because of ions at *m/z* 1107.60 and 1221.59 corresponding to $[GA\text{-}H]^-$ and $[GA+2HCOO+Na]^-$, respectively. Notably, an unknown doubly charged anion with the same *m/z* value as monoisotopic peak as $[GA\text{-}H]^-$ eluted together with it. According to the isotope distribution shown in Figure 1b, it may be $[2GA\text{-}2H]^{2-}$ or the anion of another constituent: neither could be confirmed with the current data. Other multiply-charged anions were spread over three disparate regions of the mass spectra of peak I (Figure 1b). Located at region 1, doubly charged anions at *m/z* 553.29, 576.30, and 599.30 corresponding to $[GA\text{-}2H]^{2-}$, $[GA\text{-}H+HCOO]^{2-}$, and $[GA+2HCOO]^{2-}$, respectively, originate with GA based on previous studies [16, 23]. The *m/z* of doubly and triply charged anions, located at regions 2 and 3, was greater than the molecular weight of GA and seems numerically related. We tentatively characterized ginsenoside-B (GB) from the $[GB\text{-}H]^-$ ion at *m/z* 945.54 and $[GB+HCOO]^-$ ion at *m/z* 991.55. Similarly, $[GB\text{-}H]^-$ was accompanied with a doubly charged anion possessing the same *m/z* value of the monoisotopic peak (Figure 1c). Other multiply-charged anions were found with *m/z* values at 1400–3000 Da. The multiply-charged anions also displayed a numerical relationship to GB.

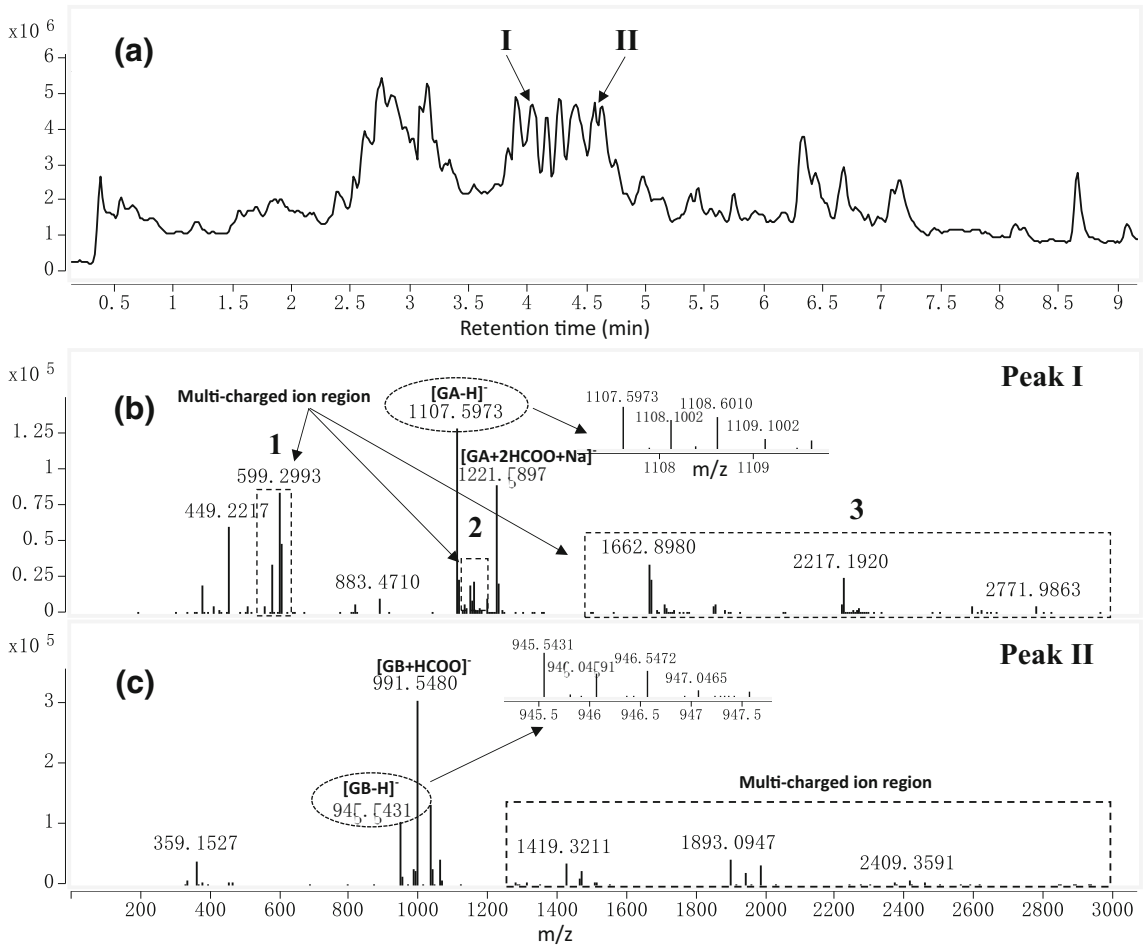

Figure 1. Total ion chromatogram of ginseng extracts (**a**) and mass spectra of peak I (**b**) and II (**c**). The retention times at 3.5~5 min were a major period that ginsenosides were eluted, so we selected peaks I (t_R = 4.08 min) and II (t_R = 4.58 min) to show the multicharged ions co-eluting with ginsenosides. $[M-H]^-$ at *m/z* 1107.5973 and 945.5431 were corresponded to ginsenoside-A (GA) and ginsenoside-B (GB), and the regions of multiply-charged anions were marked

Formation of multicharged ions is a feature of electrospray ionization, allowing macromolecular compounds with a molecular weight of 10,000 Da or more to be measured by mass analyzers with a low range of mass-to-charge ratios (usually less than 2000 Da). Indeed, macromolecules such as polypeptides, polysaccharides, and proteins have already been isolated and identified in PG and they produced multicharged ions by electrospray ionization. However, their retention times should differ from those of ginsenosides due to different polarities; co-elution with ginsenosides is unlikely.

It was worth mentioning that the molecular weight of ginsenoside is less than 1500 Da in general; thus, the mass range was commonly set within 1500 or 2000 Da as the upper limit in the previous studies. In our experiment, the TOF analyzer scanned over a mass range of *m/z* 50–3000, allowing us to collect more *m/z* information for multiply-charged anions. Based on our experimental results, formation of the multiply-charged ions may be related to co-eluting ginsenosides. We discuss their attribution and propose a mechanism for their formation in the following sections.

Various Anions of Ginsenosides in the ESI-MS Negative Ion Mode

To investigate the formation of the multiply-charged anions that co-eluted with ginsenosides, a total of 14 ginsenoside reference standards containing all the major aglycones of ginsenosides were selected and analyzed using the UPLC-ESI-HRMS system (Figure 2). The ginsenosides were classified as following: Rb_1, Rb_3, Rg_3, F_2, Rh_2, CK, and notoginsenoside Ft_1 as PPD-type ginsenosides; Re, Rf, Rg_1, Rg_2, and notoginsenoside R_1 as PPT-type ginsenosides; Ro as an oleanane-type ginsenoside; and pseudoginsenoside F_{11} as an occotillol-type ginsenoside.

On the basis of the number and substituent positions of their sugar moieties, 14 ginsenosides were divided into six categories: (i) monosaccharide ginsenosides including Rh_2 and CK; (ii) disaccharide monodesmosidic ginsenosides including Rf, Rg_2, Rg_3, and pseudoginsenoside F_{11}; (iii) disaccharide bidesmosidic ginsenosides including Rg_1 and F_2; (iv) trisaccharide monodesmosidic ginsenosides including notoginsenoside Ft_1; (v) trisaccharide bidesmosidic ginsenosides including Re, Ro,

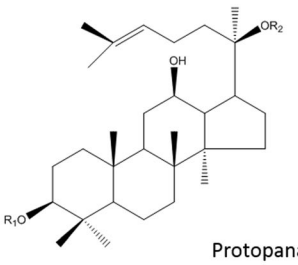

Protopanaxadiol type

Name	R1	R2	Formula
Ginsenoside Rb_1	Glc^2-Glc	Glc^6-Glc	$C_{54}H_{92}O_{23}$
Ginsenoside Rb_3	Glc^2-Glc	Glc^6-Xyl	$C_{53}H_{90}O_{22}$
Ginsenoside Rg_3	Glc^2-Glc	H	$C_{42}H_{72}O_{13}$
Ginsenoside F2	Glc	Glc	$C_{42}H_{72}O_{13}$
Ginsenoside Rh2	Glc	H	$C_{36}H_{62}O_8$
Ginsenoside C-K	H	Glc	$C_{36}H_{62}O_8$
Notoginsenoside Ft1	Glc^2-Glc^2-Xyl	H	$C_{47}H_{80}O_{17}$

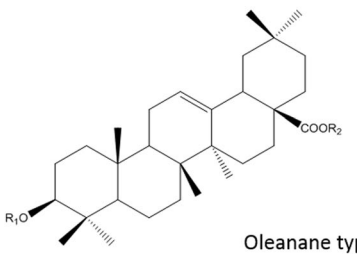

Oleanane type

Name	R1	R2	Formula
Ginsenoside R_0	$GlcA^2$-Glc	Glc	$C_{48}H_{76}O_{19}$

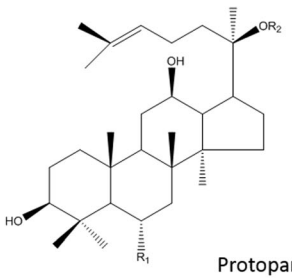

Protopanaxatriol type

Name	R1	R2	Formula
Ginsenoside Re	Glc^2-Rha	Glc	$C_{48}H_{82}O_{18}$
Ginsenoside Rf	Glc^2-Glc	H	$C_{42}H_{72}O_{14}$
Ginsenoside Rg_1	Glc	Glc	$C_{42}H_{72}O_{14}$
Ginsenoside Rg_2	Glc^2-Rha	H	$C_{42}H_{72}O_{13}$
Notoginsenoside R1	Glc^2-Xyl	Glc	$C_{47}H_{80}O_{18}$

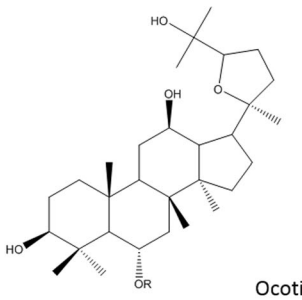

Ocotillol type

Name	R	Formula
Pseudoginsenoside F11	Glc^2-Rha	$C_{42}H_{72}O_{14}$

Glc=β-D-glucose
Xyl=β-D-xylose
Rha=α-L-rhamnose
GlcA=β-D-glucuronide

Figure 2. Structures for 14 ginsenosides used as reference substances in this study. Ginsenosides Rb_1, Rb_3, Rg_3, F_2, Rh_2, CK, and notoginsenoside Ft_1 are PPD type; Re, Rf, Rg_1, Rg_2, and notoginsenoside R_1 are PPT type; Ro is an oleanane type; and pseudoginsenoside F_{11} is an occotillol type

and notoginsenoside R_1; and (vi) tetrasaccharide bidesmosidic ginsenosides including Rb_1 and Rb_3.

Pure ginsenoside standards and mixtures were analyzed under the same chromatography and mass spectrometry conditions. Retention times for the ginsenoside standards ranged from 2.94 to 6.86 min, with the region at 3.5–5 min a major elution area for ginsenosides (Figure 3a). The compound named GA (shown in Figure 1b) was identified as Rb_1 by comparison with the pure ginsenoside. A total of 30 anions were attributable to Rb_1 including as many as 23 multicharged ions. The major anions of Rb_1 and the pattern of the isotopic distribution of 23 multicharged anions are shown in Figure 3b and Figure 4, respectively.

As summarized in Table 1 and Figure 5, dozens of anions, numerous doubly charged anions, and a handful of triply charged anions were detected in the full mass spectra of each ginsenoside. More specifically, singly-charged anions included deprotonated ions $[M-H]^-$, adduct ions $[M+Adduct]^-$ ($[M+Cl]^-$, $[M+HCOO]^-$, and $[M+2HCOO+Na]^-$), non-covalent multimer ions $[nM-H]^-$ ($[2M-H]^-$ and $[3M-H]^-$), and their anionic attachments $[nM+Adduct]^-$ ($[2M+Cl]^-$, $[2M+HCOO]^-$, $[2M+2HCOO+Na]^-$, $[3M+Cl]^-$, and $[3M+HCOO]^-$). The doubly charged anions detected in this study could be divided into two subclasses: (i) I-type doubly charged anions $[M-2H]^{2-}$ and $[M+Adduct]^{2-}$, including $[M-2H]^{2-}$, $[M-H+HCOO]^{2-}$ and $[M+2HCOO]^{2-}$, $[M-H+Cl]^{2-}$, $[M+2Cl]^{2-}$, and $[M+HCOO+Cl]^{2-}$, were formed from one ginsenoside molecule, with isotopic patterns monotonically decreasing from left to right with an isotopic variation of 0.5 Da (Figure 4a–f) and (ii) II-type doubly charged anions $[nM-2H]^{2-}$ and $[nM-H+Adduct]^{2-}$ composed of multiple ginsenoside molecules including $[2M-2H]^{2-}$, $[3M-2H]^{2-}$, $[4M-2H]^{2-}$, $[5M-2H]^{2-}$, $[6M-2H]^{2-}$, $[7M-2H]^{2-}$, $[2M-H+Cl]^{2-}$, $[3M-H+Cl]^{2-}$, $[4M-H+Cl]^{2-}$, $[5M-H+Cl]^{2-}$, $[6M-H+Cl]^{2-}$, $[7M-H+Cl]^{2-}$, $[2M-H+HCOO]^{2-}$, $[3M-H+HCOO]^{2-}$, $[4M-H+HCOO]^{2-}$, $[5M-H+HCOO]^{2-}$, $[6M-H+HCOO]^{2-}$, $[7M-H+HCOO]^{2-}$, $[2M-H+2HCOO+Na]^{2-}$, $[3M-H+2HCOO+Na]^{2-}$, $[4M-H+2HCOO+Na]^{2-}$, $[5M-H+2HCOO+Na]^{2-}$, $[6M-H+2HCOO+Na]^{2-}$, and $[7M-H+2HCOO+Na]^{2-}$. The isotope shapes of these ginsenoside patterns were Gaussian with an isotopic variation of 0.5 Da (Figure 4g–u). When $[M-H]^-$ and $[2M-2H]^{2-}$, $[2M-H]^-$ and $[4M-2H]^{2-}$, and $[3M-H]^-$ and $[6M-2H]^{2-}$ coexisted, their monoisotopic peaks had the same *m/z* values, resulting in three sets of superimposed isotope peaks that were jagged from left to right: that is, a high and low scattered arrangement of isotopic

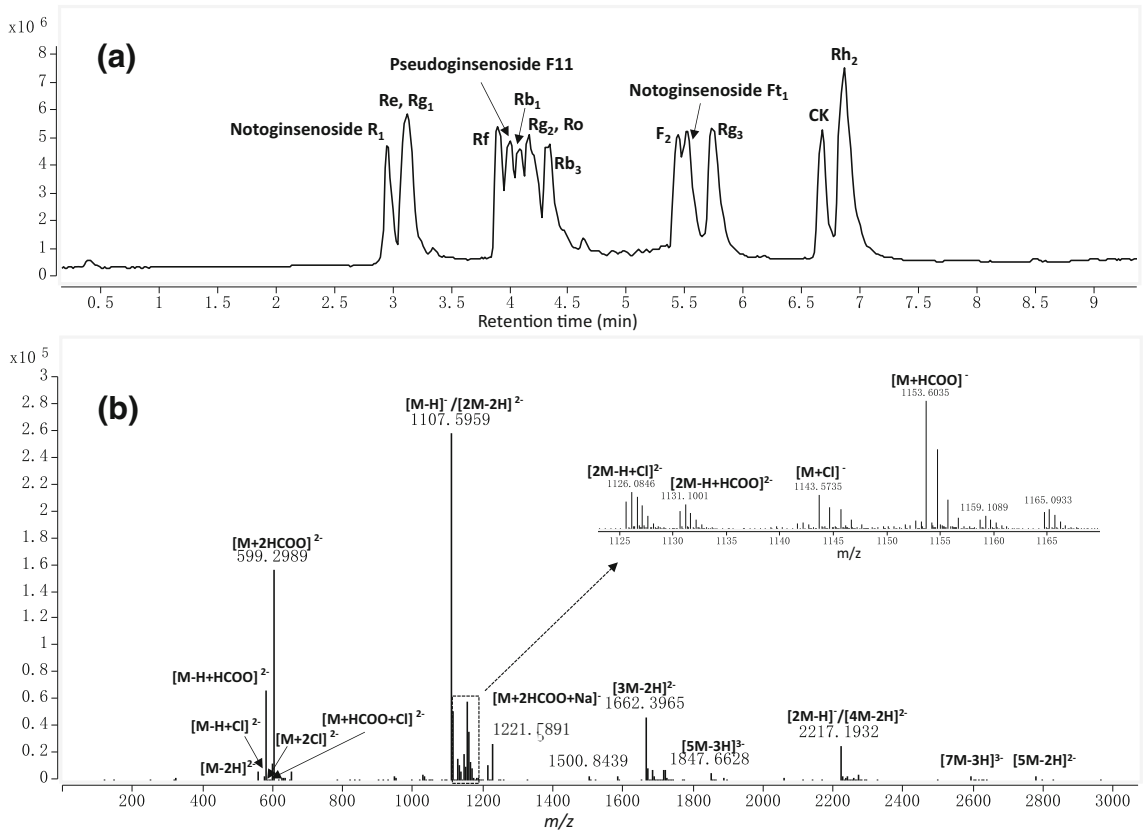

Figure 3. Total ion chromatogram of mixture of 14 ginsenoside standards (**a**) and mass spectrum of Rb_1 (**b**). A total of 30 anions were attributable to Rb_1 and 19 major anions were marked

distribution. Moreover, the triply charged anions $[nM\text{-}3H]^{3-}$ which included $[5M\text{-}3H]^{3-}$ and $[7M\text{-}3H]^{3-}$, had the same isotopic distribution as that of II-type doubly charged anions (Figure 4v, w). Normally, the mass accuracy of measured ions should be better than 10 ppm during the MS analysis for the QTOF instrument and this standard is used to control the mass accuracy of anions reported in this paper. The mass error (ppm) of each anion is less than 10 ppm, and in fact most are better than

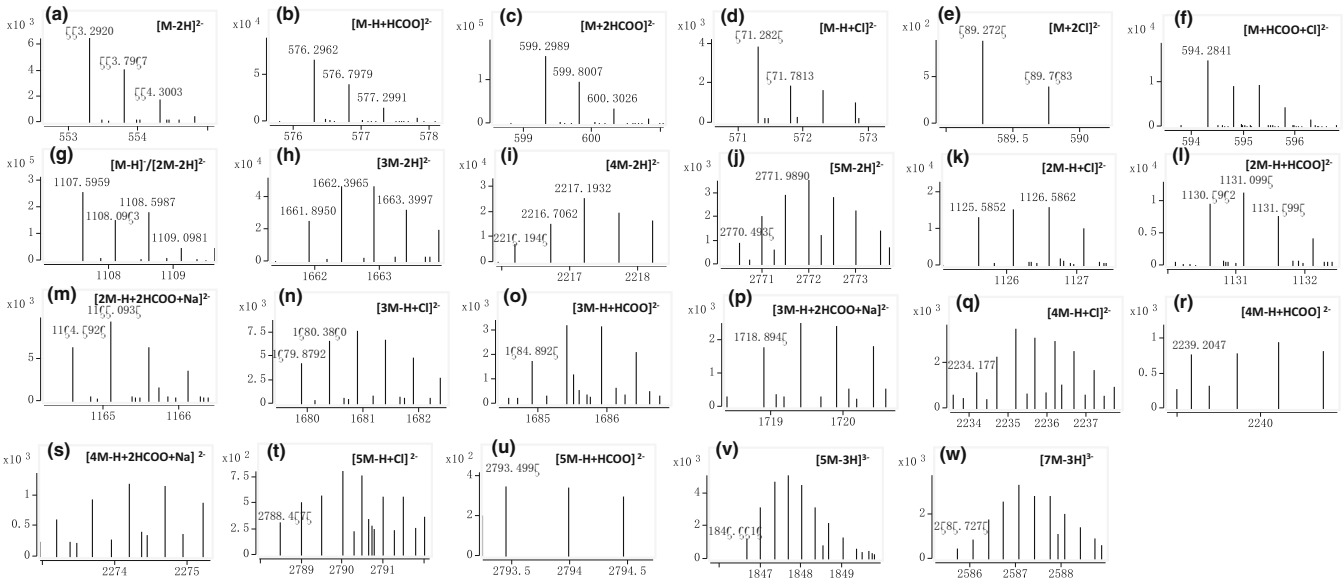

Figure 4. The isotopic distribution of 23 multicharged anions of Rb_1. The isotope shape of these anions were Gaussian distribution or half Gaussian distribution with isotopic variation of 0.5 Da. Particularly, when $[M\text{-}H]^-$ and $[2M\text{-}2H]^{2-}$, $[2M\text{-}H]^-$ and $[4M\text{-}2H]^{2-}$, and $[3M\text{-}H]^-$ and $[6M\text{-}2H]^{2-}$ coexisted, a high and low scattered arrangement of isotopes distribution were shown

Table 1. Anions of Pure Ginsenosides Detected in the Negative Ion Mode and the Percent Relative Intensity of Detected Ions vs. Base Peak

Ginsenoside (M)	G-Rb_1	G-Rb_3	G-Ro	G-Re	N-R_1	N-Ft_1	G-Rg1	G-Rf
$[M-H]^-$	1107.5956 (100)	1077.5864 (100)	955.4917 (100)	945.5435 (8.37)	931.5285 (20.17)	915.5318 (5.37)	799.4852 (0.33)	799.4852 (34.65)
$[M+Cl]^-$	1143.5740 (9.31)	1113.5599 (10.48)	991.4693 (4.51)	981.5198 (7.13)	967.5043 (11.50)	951.5089 (6.12)	835.4623 (8.09)	835.4617 (9.53)
$[M+HCOO]^-$	1153.6027 (25.21)	1123.5913 (51.69)	ND	991.5474 (100)	977.5324 (100)	961.5363 (100)	845.4883 (100)	845.4893 (100)
$[M+2HCOO+Na]^-$	1221.5891 (8.12)	1191.5781 (13.79)	1069.4840 (6.00)	1059.5357 (14.15)	1045.5209 (18.20)	1029.5250 (16.22)	913.4778 (30.54)	913.4774 (36.63)
$[2M-H]^-$	2216.1946 (3.70)	2156.1703 (5.43)	1911.9839 (5.63)	1892.0879 (1.67)	1864.0609 (6.25)	1832.0687 (14.31)	1599.9783 (5.29)	1599.9754 (48.02)
$[2M+Cl]^-$	2252.1727 (0.20)	2192.1543 (0.30)	ND	1928.0655 (0.35)	1900.0375 (0.47)	1868.0453 (0.89)	1635.9535 (0.37)	1635.9516 (3.65)
$[2M+HCOO]^-$	2262.2025 (0.19)	2202.1982(0.15)	ND	1938.0953 (0.55)	1910.0662 (0.93)	1878.0695 (0.70)	1645.9808 (1.71)	1645.9801 (1.15)
$[2M+2HCOO+Na]^-$	ND	ND	ND	ND	1978.0598 (0.08)	1946.0575 (0.11)	ND	1713.9702(0.14)
$[3M-H]^-$	OR	OR	ND	ND	ND	2748.5955 (0.29)	2400.4607(0.09)	2400.4585 (0.64)
$[3M+Cl]^-$	OR	OR	ND	ND	ND	2784.5828 (0.03)	2436.4443 (0.02)	2436.4467 (0.07)
$[3M+HCOO]^-$	OR	OR	ND	ND	ND	ND	2446.4615 (0.04)	2446.4745 (0.03)
$[3M+2HCOO+Na]^-$	OR	OR	ND	ND	ND	ND	ND	ND
$[M-2H]^{2-}$	553.2935 (3.33)	538.2884 (0.98)	ND	ND	ND	ND	ND	ND
$[M-H+HCOO]^{2-}$	576.2970 (25.83)	561.2918 (16.02)	500.2441 (7.50)	495.725 (0.05)	488.2614 (0.22)	ND	ND	ND
$[M+2HCOO]^{2-}$	599.2996 (61.57)	584.2951 (40.08)	ND	518.2746 (0.15)	511.2640 (0.39)	ND	ND	ND
$[M-H+Cl]^{2-}$	571.2825 (1.62)	556.2772 (0.89)	495.2251(0.50)	ND	ND	ND	ND	ND
$[M+2Cl]^{2-}$	589.2725 (0.51)	574.2616 (0.36)	ND	ND	ND	ND	ND	ND
$[M+HCOO+Cl]^{2-}$	594.2831 (6.08)	579.277 (4.14)	ND	513.2605 (0.04)	506.2475 (0.11)	ND	ND	ND
$[2M-2H]^{2-a}$	1108.0964 (58.42)	1078.0882 (60.80)	955.9925 (40.77)	946.0438 (0.54)	932.0306 (12.37)	ND	799.9839 (0.11)	ND
$[2M-H+Cl]^{2-}$	1125.5823 (5.71)	1095.5743 (4.95)	ND	ND	949.5185 (0.90)	ND	817.4665 (0.08)	ND
$[2M-H+HCOO]^{2-}$	1130.5962 (4.30)	1100.5893 (5.06)	ND	968.5478 (0.34)	954.5352 (0.30)	ND	822.4876 (0.46)	ND
$[2M-H+2HCOO+Na]^{2-}$	1164.5926 (3.45)	1134.5805 (2.71)	ND	ND	ND	ND	ND	ND
$[3M-2H]^{2-}$	1661.8956 (9.93)	1616.8834 (12.82)	1433.7424 (19.52)	1418.8174 (1.65)	1397.7974 (3.68)	ND	1199.728 (0.58)	ND
$[3M-H+Cl]^{2-}$	1679.8792 (2.44)	1634.8746 (1.65)	ND	1436.8121 (0.36)	1415.7798 (0.17)	ND	1217.7155 (0.17)	ND
$[3M-H+HCOO]^{2-}$	1684.8925 (0.68)	1639.8816 (1.05)	ND	1441.8176 (0.93)	1420.7951 (0.74)	ND	1222.7339 (0.61)	ND
$[3M-H+2HCOO+Na]^{2-}$	1718.8945 (0.55)	1673.8785 (0.72)	ND	1475.8085 (0.08)	1454.7879 (0.08)	ND	1256.7266 (0.02)	ND
$[4M-2H]^{2-a}$	2216.7057 (7.15)	2156.6873 (11.85)	1912.4899 (7.18)	1892.5907 (1.53)	1864.5600 (4.53)	1832.5555 (1.23)	1600.4783 (1.16)	ND
$[4M-H+Cl]^{2-}$	2234.1770 (0.54)	2174.1683 (0.74)	ND	1910.0809 (0.24)	1882.0532 (0.47)	1850.0621 (0.05)	1617.9655 (0.14)	ND
$[4M-H+HCOO]^{2-}$	2239.2047 (0.28)	2179.1725 (0.26)	ND	1915.0925 (0.31)	1887.0543 (0.47)	ND	1622.9818 (0.39)	ND
$[4M-H+2HCOO+Na]^{2-}$	2273.2082 (0.16)	2213.175 (0.22)	ND	1949.0710 (0.09)	1921.0419 (0.09)	ND	1656.9815 (0.04)	ND
$[5M-2H]^{2-}$	2770.4935 (0.39)	2695.4568 (0.59)	2390.2511 (0.15)	2365.3635 (0.10)	2330.3235 (0.35)	2290.3315 (0.51)	2000.2173 (0.30)	ND
$[5M-H+Cl]^{2-}$	2788.4977 (0.15)	2713.4619 (0.17)	ND	2383.3572 (0.08)	2348.3035 (0.11)	2308.3396 (0.09)	ND	ND
$[5M-H+HCOO]^{2-}$	2793.4995 (0.09)	2718.4633 (0.14)	ND	2388.3575 (0.09)	2353.3135 (0.12)	ND	ND	ND
$[5M-H+2HCOO+Na]^{2-}$	ND	ND	ND	2433.3480 (0.05)	2387.3233(0.04)	ND	ND	ND
$[6M-2H]^{2-a}$	OR	OR	ND	ND	ND	2749.1229 (0.49)	2400.9740 (0.16)	2400.9623 (0.59)
$[6M-H+Cl]^{2-}$	OR	OR	ND	ND	ND	2766.6164 (0.05)	2418.4600 (0.05)	2418.4621 (0.07)
$[6M-H+HCOO]^{2-}$	OR	OR	ND	ND	ND	ND	ND	ND
$[6M-H+2HCOO+Na]^{2-}$	OR	OR	ND	ND	ND	ND	ND	ND
$[7M-2H]^{2-}$	OR	OR	OR	OR	OR	OR	2800.7102 (0.02)	2800.7062 (0.15)
$[7M-H+Cl]^{2-}$	OR	OR	OR	OR	OR	OR	ND	ND
$[7M-H+HCOO]^{2-}$	OR	OR	OR	OR	OR	OR	ND	ND
$[7M-H+2HCOO+Na]^{2-}$	OR	OR	OR	OR	OR	OR	ND	ND
$[5M-3H]^{3-}$	1846.6616 (0.49)	1796.6342 (0.18)	ND	ND	ND	ND	ND	ND
$[7M-3H]^{3-}$	2585.7275 (0.45)	2515.7302 (0.13)	2230.8090 (0.47)	2207.6065 (0.03)	2174.8971 (0.07)	ND	1866.7924(0.03)	ND

Ginsenoside (M)	G-Rb_1	G-Rg_3	G-CK	G-Rh_2
$[M-H]^-$	1107.5956 (100)	783.4900 (16.80)	621.4372 (0.43)	621.4358 (0.14)
$[M+Cl]^-$	1143.5740 (9.31)	819.4666 (7.05)	657.4132 (9.93)	657.4133 (6.40)
$[M+HCOO]^-$	1153.6027 (25.21)	829.4946 (100)	667.4417 (100)	667.4441 (100)

Table 1 (continued)

Ginsenoside (M)	G-Rb_1	G-Rg_3	G-CK	G-Rh_2
$[M+2HCOO+Na]^-$	1221.5891 (8.12)	897.4826 (38.58)	735.4293 (3.70)	735.4296 (6.52)
$[2M-H]^-$	2216.1946 (3.70)	1567.9860 (47.08)	1243.8810 (20.59)	1243.8820 (14.15)
$[2M+Cl]^-$	2252.1727 (0.20)	1603.9617 (2.66)	1279.8582 (0.09)	1279.8582 (0.63)
$[2M+HCOO]^-$	2262.2025 (0.19)	1613.9918 (1.40)	1289.8872 (0.47)	1289.8882 (2.19)
$[2M+2HCOO+Na]^-$	ND	1681.9775 (0.22)	1357.8680 (0.02)	1357.8809 (0.02)
$[3M-H]^-$	OR	2352.4734 (1.78)	ND	1866.3213 (1.62)
$[3M+Cl]^-$	OR	2388.4614 (0.10)	ND	ND
$[3M+HCOO]^-$	OR	2398.4885 (0.05)	ND	1912.3302 (0.07)
$[3M+2HCOO+Na]^-$	OR	ND	ND	ND
$[M-2H]^{2-}$	553.2935 (3.33)	ND	ND	ND
$[M-H+HCOO]^{2-}$	576.2970 (25.83)	ND	ND	ND
$[M+2HCOO]^{2-}$	599.2996 (61.57)	ND	ND	ND
$[M-H+Cl]^{2-}$	571.2825 (1.62)	ND	ND	ND
$[M+2Cl]^{2-}$	589.2725 (0.51)	ND	ND	ND
$[M+HCOO+Cl]^{2-}$	594.2831 (6.08)	ND	ND	ND
$[2M-2H]^{2-a}$	1108.0964 (58.42)	ND	ND	ND
$[2M-H+Cl]^{2-}$	1125.5823 (5.71)	ND	ND	ND
$[2M-H+HCOO]^{2-}$	1130.5962 (4.30)	ND	ND	ND
$[2M-H+2HCOO+Na]^{2-}$	1164.5926 (3.45)	ND	ND	ND
$[3M-2H]^{2-}$	1661.8956 (9.93)	ND	ND	932.6585 (0.01)
$[3M-H+Cl]^{2-}$	1679.8792 (2.44)	ND	ND	ND
$[3M-H+HCOO]^{2-}$	1684.8925 (0.68)	ND	ND	ND
$[3M-H+2HCOO+Na]^{2-}$	1718.8945 (0.55)	ND	ND	ND
$[4M-2H]^{2-a}$	2216.7057 (7.15)	ND	ND	ND
$[4M-H+Cl]^{2-}$	2234.1770 (0.54)	ND	ND	ND
$[4M-H+HCOO]^{2-}$	2239.2047 (0.28)	ND	ND	ND
$[4M-H+2HCOO+Na]^{2-}$	2273.2082 (0.16)	ND	ND	ND
$[5M-2H]^{2-}$	2770.4935 (0.39)	1960.2315 (0.31)	ND	1555.1067(0.01)
$[5M-H+Cl]^{2-}$	2788.4977 (0.15)	1978.2088 (0.06)	ND	ND
$[5M-H+HCOO]^{2-}$	2793.4995 (0.09)	1983.2371(0.08)	ND	ND
$[5M-H+2HCOO+Na]^{2-}$	ND	ND	ND	ND
$[6M-2H]^{2-a}$	OR	2352.9759 (1.66)	ND	1866.8117(0.11)
$[6M-H+Cl]^{2-}$	OR	2370.4676 (0.12)	ND	ND
$[6M-H+HCOO]^{2-}$	OR	ND	ND	ND
$[6M-H+2HCOO+Na]^{2-}$	OR	ND	ND	ND
$[7M-2H]^{2-}$	OR	2744.7261 (0.24)	ND	2177.5424 (0.02)
$[7M-H+Cl]^{2-}$	OR	2762.6949 (0.05)	ND	ND
$[7M-H+HCOO]^{2-}$	OR	ND	ND	ND
$[7M-H+2HCOO+Na]^{2-}$	OR	ND	ND	ND
$[5M-3H]^{3-}$	1846.6616 (0.49)	ND	ND	ND
$[7M-3H]^{3-}$	2585.7275 (0.45)	ND	ND	ND

ND not detected, *OR* outrange, *G* ginsenoside, *N* notoginsenoside, *P* pseudoginsenoside

[a]Second isotope

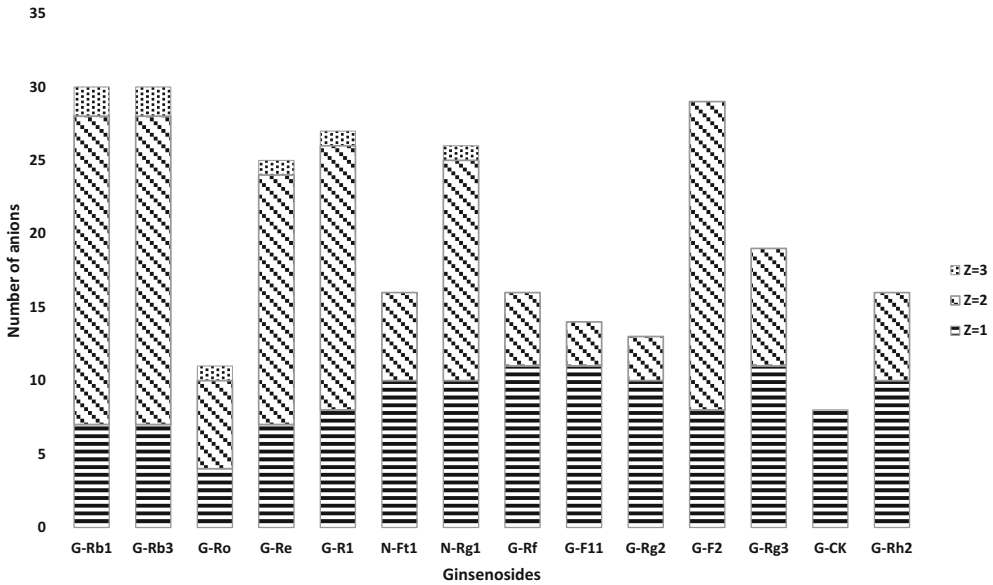

Figure 5. Comparison of the number of anions detected in 14 ginsenosides. Abundant doubly charged anions and a handful of triply charged anions with common singly charged ions were observed in the mass spectra of each ginsenoside

5 ppm (Tables A.1~14). To summarize, we have verified that multicharged ions co-eluting with ginsenosides were generated during ionization of corresponding ginsenosides.

Effect of Solution Concentration on the Anions of Ginsenoside

Ding et al. have reported that the appearance of dimer ions $[2M+H]^+$ and $[2M-H]^-$ was concentration-dependent, suggesting a non-covalent association [28]. To study the effect of the concentration on the formation mechanism for multicharged multimer anions (including $[nM-2H]^{2-}$ and $[nM-3H]^{3-}$), several ginsenoside mixtures of different concentrations were prepared.

As summarized in Tables A.15~28, ginsenoside concentration affected the formation of certain anions. Using Rb_1 to illustrate our results, as plotted in Figure 6a, common quasi-molecular ions of ginsenosides including $[M-H]^-$, $[M+Cl]^-$, and $[M+HCOO]^-$ were detected at the lowest concentration of Rb_1 (0.013 μM); the formation of these anions was not affected by the ginsenoside concentration. In addition, signal intensities of $[M-H]^-$, $[M+Cl]^-$, and $[M+HCOO]^-$ were linear at low concentrations (6.44 μM), and tended to saturate as concentration increased (Figure 6b). Moreover, the intensity of $[M+Cl]^-$ and $[M+HCOO]^-$ decreased slightly at the highest concentration (128.86 μM). A logarithmic scale describes the behavior at low concentrations (Figure 6c).

As mentioned above, formation of the non-covalent dimer anion $[2M-H]^-$ depended on concentration; ions such as $[2M-H]^-$ were detected only at relatively high ginsenoside concentrations. $[2M-H]^-$ was not observed at relatively low concentrations, but could be detected once the concentration reached a minimum level (Figure 6a). $[3M-H]^-$ ions had a similar tendency, but required a higher concentration to form than $[2M-H]^-$. Anionic adducts of $[2M-H]^-$ and $[3M-H]^-$ were also detected with the increasing concentration. Similarly, formation of $[nM-2H]^{2-}$, $[nM-3H]^{3-}$, and their anionic adducts was also concentration-dependent. As shown in Figure 6a, these multimer anions of Rb_1 were observed when ginsenoside concentration increased by at least 20 times. Higher concentrations were required to form multicharged multimers, implying that the association of $[nM-2H]^{2-}$ and $[nM-3H]^{3-}$ types is non-covalent.

Formation of Ginsenoside Anions and Relationship between Anions and Molecular Structures of Ginsenosides

As shown in Table 1, $[M-H]^-$, $[M+Cl]^-$, $[M+HCOO]^-$, and $[M+2HCOO+Na]^-$ anions were observed in the ESI-MS spectra of all ginsenosides selected in this study except for Ro ($[Ro+HCOO]^-$ was not detected). Notably, $[M+HCOO]^-$ anion base peaks were observed in the full mass spectra of the majority of ginsenosides including ginsenosides Re, Rf, Rg_1, Rg_2, Rg_3, F_2, Rh_2, CK, Ft_1, R_1, and F_{11}, whereas deprotonated anions $[M-H]^-$ were predominant in the mass spectra of Rb_1, Rb_3, and Ro.

Gasification and ionization of compounds are accomplished simultaneously during negative mode electrospray ionization, meaning that samples are directly brought into the gas phase from the solution phase by deprotonation or attachment of small anions. Thus, the ionization of samples does not depend on their volatility, but rather on their ability to bind charges [29]. The signal intensity of the dominant ion (base peak) should be higher than the others. For instance, Ro has an acidic proton in the glucuronide and can be ionized by losing the proton. In our experiment, Ro was deprotonated to form the $[Ro-H]^-$ anion at *m/z* 955.49 as the dominant ionization (100), with other subordinate ionizations such as $[Ro+Cl]^-$ at *m/z* 991.47 (4.51), $[Ro+2HCOO+Na]^-$ at *m/z* 1069.48 (6.00), and $[2Ro-H]^-$ at *m/z* 1911.98 (5.63), whereas $[Ro+HCOO]^-$ was

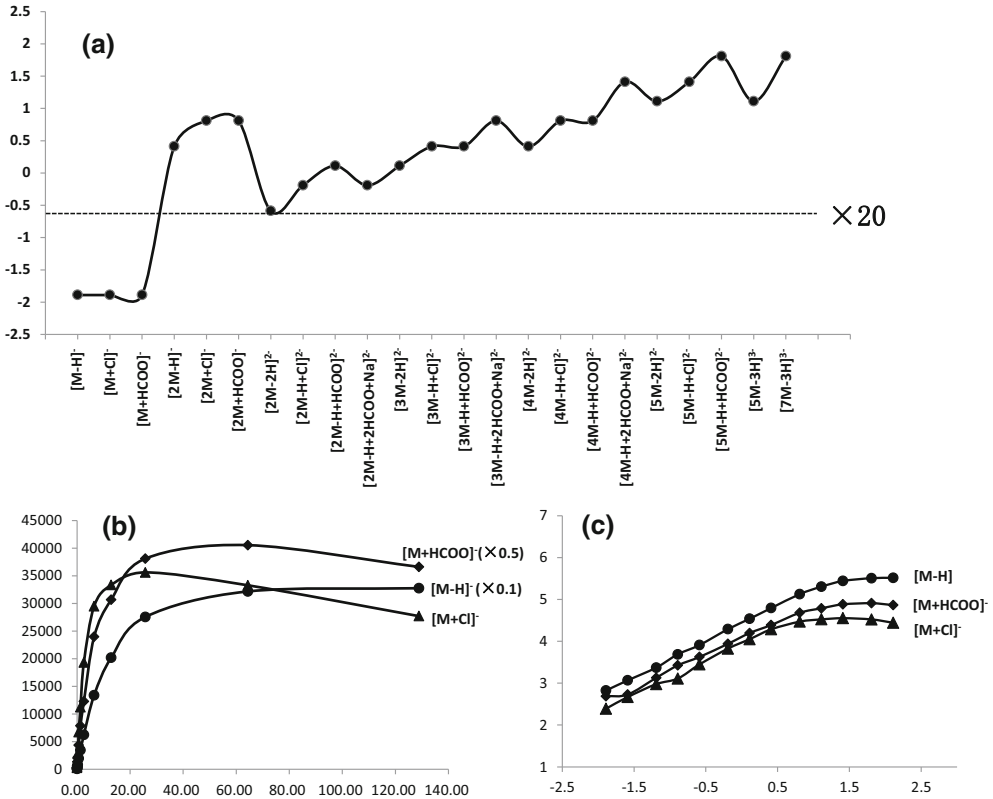

Figure 6. Formation concentration of Rb_1 anions (**a**) and effect of the solution concentration on $[M-H]^-$, $[M+Cl]^-$,and $[M+HCOO]^-$ of Rb_1 (**b**, **c**). (**a**) The formation of $[M-H]^-$, $[M+Cl]^-$, and $[M+HCOO]^-$ was not affected by the ginsenoside concentration, so formation concentration of other anions were based on this concentration as a base level. All formation concentration of mentioned multicharged anions was at least 20 times higher than the base level. Logarithmic scale chart was adopted because of the wide range of concentration. (**b**) The ion intensity of $[M-H]^-$, $[M+Cl]^-$, and $[M+HCOO]^-$ was a linear pattern in the low concentration region. However, it tended to be saturated with the increase of solution concentration. Moreover, the intensity might decrease slightly at the highest concentration. (**c**) Logarithmic scale chart could clearly describe details at low concentration area than the original curve

not detected. Except for Ro, the ginsenosides used in this study were all neutral saponins that do not readily produce $[M-H]^-$ in the negative ion mode, but can form adducts with various ions on their saccharide groups. For example, anion attachment of formate results from the mobile phase used in the analysis. Sodium and chloride (from glassware, storage bottles, or analytical grade solvents) can form adducts as well. Our results indicated that ionization of neutral ginsenosides Re, Rf, Rg_1, Rg_2, Rg_3, F_2, Rh_2, CK, Ft_1, R_1, and F_{11} occurred by formic acidification ($[M+HCOO]^-$) rather than by deprotonation ($[M-H]^-$), whereas for Rb_1 and Rb_3 both deprotonation and formic acidification occurred.

$[M-2H]^{2-}$ type anions were observed in the mass spectra of Rb_1, Rb_3, Re, Ro, and R_1. Since these ginsenosides contain a variety of aglycon types (including PPD, PPT, and oleanolic), this factor does not determine whether this type of doubly charged anions can be formed or not. Notably, these ginsenosides all are trisaccharide/tetrasaccharide bidesmosidic saponins. More specifically, at least one of the two sugar moieties attached to aglycone is a disaccharide. For instance, although F_2 and Rg_1 were bidesmosidic saponins with two glucose residues (Glc) at C3/C6 and C20, $[M-2H]^{2-}$ type anions were not detected in the mass spectra of either F_2 or Rg_1. Doubly charged ions $[M-2H]^{2-}$, $[M-H+AcO]^{2-}$, and $[M+2AcO]^{2-}$ in the ESI mass spectra of Rb_1, Rb_2, Rc, Rd, and Re were first reported by Miao et al. [23]. Ng and coworkers [16] also detected them in the full mass spectra of Rb_2, Rc, Rd, Re, and Rg_1, and noticed that the ion intensity ratio for Rg_1 was smaller than for other ginsenosides. They concluded that formation of $[M+2AcO]^{2-}$ was influenced by the chain length of glycosyl groups, and the two negative charges in $[M-H+AcO]^{2-}$ and $[M+2AcO]^{2-}$ might be located on separate glycosyl groups in order to minimize Columbic repulsion.

Notably, we discovered and first reported that $[M-H+Cl]^{2-}$, $[M+2Cl]^{2-}$, and $[M+HCOO+Cl]^{2-}$ were typically formed by some bidesmosidic ginsenosides in addition to $[M-2H]^{2-}$, $[M-H+HCOO]^{2-}$, and $[M+2HCOO]^{2-}$ anions. We noted that $[M-H+HCOO]^{2-}$ was produced by all bidesmosidic ginsenosides with at least one disaccharide moiety attached to aglycones, including Rb_1, Rb_3, Re, Ro, and R_1. $[M+2HCOO]^{2-}$ and $[M+HCOO+Cl]^{2-}$ were produced by each of these ginsenosides except for Ro. Moreover, the $[M-H+Cl]^{2-}$ ion was detected in the mass spectrum of Rb_1, Rb_3, and Ro, whereas $[M-2H]^{2-}$ and $[M+2Cl]^{2-}$ were only observed in the mass spectrum of Rb_1 and Rb_3. We attribute these results to the diverse ionization sites in this species of ginsenosides. For instance, Ro

had a very acidic proton in the glucuronide at C3, which was ionized easily by losing the proton to form $[Ro-H]^-$. Therefore, $HCOO^-$ and Cl^- could bond to Ro through the hydroxyl radical of Glc located at C20, giving rise to $[Ro-H+HCOO]^{2-}$ and $[Ro-H+Cl]^{2-}$, respectively. $[Ro+2HCOO]^{2-}$, $[Ro+2Cl]^{2-}$, and $[Ro+HCOO+Cl]^{2-}$ were not observed, due to the shortage of reaction sites. Remarkably, $[M-2H]^{2-}$ was not produced with Ro, but was observed in the mass spectra of Rb_1 and Rb_3, each of which contains two disaccharide moieties on their aglycones. As mentioned previously, deprotonation was the predominant ionization for the disaccharide moiety of ginsenosides including Rb_1 and Rb_3 and, in general, the ion intensity ratio, $I_{[M-H]^-}/I_{[M+HCOO]^-}$, of ginsenosides with a disaccharide moiety was higher than that of monosaccharide group(s). This suggests that the chain length of the saccharide moiety is one key factor in the deprotonation of ginsenosides. In summary, $[M-2H]^{2-}$-type anions including $[M-2H]^{2-}$, $[M-H+HCOO]^{2-}$, $[M+2HCOO]^{2-}$, $[M-H+Cl]^{2-}$, $[M+2Cl]^{2-}$, and $[M+HCOO+Cl]^{2-}$ were produced by tetrasaccharide bidesmosidic ginsenosides including Rb_1 and Rb_3, while $[M-H+HCOO]^{2-}$, $[M+2HCOO]^{2-}$, and $[M+HCOO+Cl]^{2-}$ were formed by tetrasaccharide bidesmosidic neutral ginsenosides including Re and R_1.

Under our experimental conditions, doubly charged multimer anions $[2M-2H]^{2-}$ and $[3M-2H]^{2-}$ were only simultaneously observed in the full mass spectra of bidesmosidic ginsenosides Rb_1, Rb_3, Re, F_2, Rg_1, Ro, and R_1, respectively. In addition, $[4M-2H]^{2-}$ ions also were detected in the mass spectra of Ft_1, a trisaccharide monodesmosidic ginsenoside. $[5M-2H]^{2-}$ ions were detected in the mass spectra of Rg_3, Rh_2, and the eight previously mentioned ginsenosides, respectively. Moreover, $[6M-2H]^{2-}$ and $[7M-2H]^{2-}$ were produced by Rf, Rg_1, Rg_2, Rg_3, Rh_2, F_2, F_{11}, and Ft_1 (the weak intensity of $[3Rh_2-2H]^{2-}$ required magnification to be viewed). Doubly charged multimer anions of $[nM-2H]^{2-}$ type did not appear in the mass spectrum of CK. $[nM-H+Adduct]^{2-}$ ions were observed in the full mass spectra of certain ginsenosides. The patterns for these anions are similar to those of $[nM-2H]^{2-}$.

The above experimental results demonstrate that formation of II-type doubly charged anions have certain regularities. Firstly, $[2M-2H]^{2-}$ and $[3M-2H]^{2-}$ can be generated simultaneously by ginsenosides containing two sugar chains (glycosyl groups at two sites of aglycon), whatever the saccharide composition of the saponins. These ginsenosides include tetrasaccharide bidesmosidic ginsenosides (Rb_1 and Rb_3), trisaccharide bidesmosidic ginsenosides (Re, Ro, and notoginsenoside R_1), and disaccharide bidesmosidic ginsenosides (Rg_1 and F_2). Thus, monodesmosidic and/or bidesmosidic ginsenosides can be rapidly identified by using mass spectra to identify joint diagnostic anions $[2M-2H]^{2-}$ and $[3M-2H]^{2-}$. Secondly, more molecules (M) of monodesmosidic ginsenosides are required to form $[nM-2H]^{2-}$ anions compared to those in the bidesmosidic group, regardless of the number of saccharides comprising the ginsenosides. For example, although comprised of three sugars (Glc-Glc-Xyl), Ft_1 cannot produce $[2M-2H]^{2-}$ and $[3M-2H]^{2-}$ due to the single sugar chain. In fact, at least four molecules were required to form $[nM-2H]^{2-}$ for Ft_1. Thirdly, ginsenosides with sugar moieties attached to the hydroxyl at C-3 form $[nM-2H]^{2-}$ anions more readily than those with sugar moieties at C-6, and ginsenosides with a single sugar moiety attached to the C-20 hydroxyl might not produce the $[nM-2H]^{2-}$ anions. The following examples of several groups of isomers illustrated these conclusions preferably.

Rh_2 and CK, PPD isomers of monodesmosidic ginsenosides, are rare [30]. Rh_2 has shown beneficial pharmacology such as anti-tumor and anti-fatigue effects [31], but is found only in small quantities in red ginseng and wild ginseng. CK is a main degradation product of natural PPD-type ginsenosides (such as Rb_1, Rb_2, and Rc) produced by human intestinal bacteria. It is the major form of ginsenoside absorbed by the body and can be transformed from ginsenoside by food micro-organisms in vitro, with multifarious bioactivities including anti-inflammation, liver protection, and bone marrow depression reduction. Rh_2 and CK are characterized by the position of their glucose moieties. Rh_2 is a ginsenoside with a glucose moiety attached to the β-OH at C-3, while CK has a glucose moiety on the β-OH at C-20. $[3M-2H]^{2-}$, $[5M-2H]^{2-}$, $[6M-2H]^{2-}$, and $[7M-2H]^{2-}$ were observed in the mass spectra of Rh_2, but no $[nM-2H]^{2-}$ anions were found in the mass spectra of CK. Therefore, Rh_2 and CK can be quickly and effectively distinguished with full mass spectrum analysis at a mass range of *m/z* less than 3000 using multicharged multimer anions as diagnostic anions.

Rg_1, Rf, and F_{11} are disaccharide isomers, sharing the same molecular formula ($C_{42}H_{72}O_{34}$). Of all ginsenosides, Rg_1 is one of the most important, having a variety of pharmacological activities such as irritant effects on the central nervous system, memory enhancement, and anti-fatigue. Rf and F_{11} are two powerful marker compounds for the identification of PG and PQ, because F_{11} is only found in PQ, whereas Rf is present in PG and absent in PQ [32]. Rg_1 and Rf are both PPT-type ginsenosides, and F_{11} is an ocotillol type. Rg_1 is linked to the α-OH at C-6 and C-20 with Glc, respectively. Rf and pseudoginsenoside F_{11} are linked to the α-OH at C-6 with Glc-Glc and Glc-Rha, respectively. $[2M-2H]^{2-}$, $[3M-2H]^{2-}$, and $[4M-2H]^{2-}$ were only observed in the mass spectra of Rg_1, a bidesmosidic ginsenoside, while monodesmosidic ginsenosides Rf and F_{11} did not produce these ions. Rf and F_{11} (linked to the α-OH at C-6 with disaccharide) produced $[6M-2H]^{2-}$ and $[7M-2H]^{2-}$ despite different compositions in their sugar moieties. Notably, there were significant differences in the ion intensity ratio, $I_{[6M-2H]^{2-}}/I_{[M+HCOO]^-}$ and $I_{[M-H]^-}/I_{[M+HCOO]^-}$, between Rf (0.59, 34.65) and F_{11} (0.04, 5.41) which could differentiate these two isomeric ginsenosides.

F_2, Rg_2, and Rg_3 are another group of isomeric compounds containing two sugars. Rg_3 and F_2 are both PPD-type ginsenosides. The former has Glc-Glc attached to the β-OH at C-3 and the latter has Glc linked to the β-OH at C-3 and C-20. Rg_2 is a PPT-type ginsenoside with Glc-Glc linked to the α-OH at C-6 in the aglycon. The formation of $[nM-2H]^{2-}$ anions differed among them. Except for Rg_2 and Rg_3, $[2M-2H]^{2-}$, $[3M-2H]^{2-}$, and $[4M-2H]^{2-}$ were only observed in the mass

spectra of F_2, the bidesmosidic ginsenoside. In addition to F_2, $[5M-2H]^{2-}$ could also be observed in the mass spectra of Rg_3, the PPD-type ginsenoside. However, six Rg_2 molecules were required to form of this doubly charged anion because of the aglycone PPT.

In conclusion, the number and substitution positions of the sugar moieties are key factors influencing the formation of the $[nM-2H]^{2-}$ anions. Essentially, the hydroxyl groups of ginsenosides as reactive groups on glycosyl are the decisive factor for the formation of these type anions of ginsenosides. $[5M-3H]^{3-}$ and $[7M-3H]^{3-}$ ions were observed in the mass spectra of Rb_1 and Rb_3. In addition, $[7M-3H]^{3-}$ ions were also observed in the mass spectra of ginsenoside Re, Rg_1, Ro, and R_1. Similar to II-type doubly charged ions, when fewer aglycons comprise the ginsenosides, more molecules are required to form triply charged ions.

CID of Ginsenosides Anions in the Negative Ion Mode

Tandem mass spectrometry analysis (MS/MS) of ginsenosides was an effective method to elucidate and characterize the structures of these triterpene saponins and was used for combination analysis of ions formed in the electrospray ionization source by CID. CID is capable of dissociating weak bonds, particularly those associated with non-covalent binding. In a typical experiment, ginsenoside sugar units were successively or simultaneously lost from the deprotonated precursors $[M-H]^-$ by CID. The neutral loss of 162, 146, 132, and 176 Da mass units was attributed to the elimination of Glc, Rha, Ara (or Xyl), and Glur A residues, respectively. In addition, the product ions with *m/z* 459.38, 475.38, and 455.35 were diagnostic daughter ions corresponding to PPD, PPT, and oleanane, respectively. Moreover, characteristic ions distributed in the low mass region ($m/z < 300$) were produced from the cleavage of sugar residues, providing more structural information about the saccharide moiety. The fragmentation behavior of ginsenosides was studied by changing CID voltage among a wide range from 5 to 80 V. In general, larger ginsenoside molecules required greater CID voltage to product fragment ions.

Aimed to deduce the regular fragmentation pathways of $[nM-2H]^{2-}$, precursors $[3M-2H]^{2-}$, $[5M-2H]^{2-}$, and/or $[7M-2H]^{2-}$ of ginsenosides which could be generated were subjected to a series of CID experiments with energies ranging from 5 to 80 V (monoisotopic peaks of $[M-H]^-/[2M-2H]^{2-}$, $[2M-H]^-/[4M-2H]^{2-}$, $[3M-H]^-/[6M-2H]^{2-}$ had the same *m/z* values, which made the results complex and confused). As mentioned before, $[2F_2-2H]^{2-}$ and $[3F_2-2H]^{2-}$ could be simultaneously observed just only in the mass spectra of bidesmosidic ginsenosides, while $[4F_2-2H]^{2-}$, $[5F_2-2H]^{2-}$, $[6F_2-2H]^{2-}$, and $[7F_2-2H]^{2-}$ could be partially or wholly produced by both monodesmosidic and bidesmosidic ginsenosides. Notably, we discovered that the product ion mass spectra of monodesmosidic and bidesmosidic ginsenosides were also significantly different. Ginsenoside F_2 was taken as an example to illustrate the CID fragmentation behavior of bidesmosidic ginsenosides. Product ion mass spectra of $[3F_2-2H]^{2-}$ at *m/z* 1175.74 are shown in Figure 7. Using a collision energy of 5 V, we observed the $[3F_2-2H]^{2-}$ precursor ion as well as a weak intensity daughter ion at *m/z* 783.49, corresponding to $[2F_2-2H]^{2-}$. Increasing the collision energy from 5 to 15 V resulted in a larger ion intensity ratio, $I_{[2F2-2H]}{}^{2-}/I_{[3F2-2H]}{}^{2-}$, and the appearance of $[2F_2-H]^-$. With collision energies up to 30 V, weak signals of daughter ions at *m/z* 621.44 and 459.37 (corresponding to $[F_2-H-Glc]^-$ and $[F_2-H-Glc-Glc]^-$, respectively) were produced by loss of Glc units successively or simultaneously. Since a dissociation voltage of 30 V was sufficient to break covalent bonds in F_2, lower energies are required to cleave weaker non-covalent bonds. Notably, a doubly charged product ion at *m/z* 702.46 was observed with a collision energy of 30 V; this may correspond to $[2F_2-2H-Glc]^{2-}$. The $[3F_2-2H]^{2-}$ precursor was significantly degraded into $[2F_2-2H]^{2-}$ and/or other product ions with collision energies in the range of 35–80 V. Based on isotopic distribution and ratio, $[2F_2-2H]^{2-}$ coexisted with $[F_2-H]^-$ and the intensity of $[F_2-H-Glc]^-$, $[F_2-H-Glc-Glc]^-$, and other fragment ions formed from the cleavage of sugar residues distributed in the low mass region gradually increased with energies between 40 and 55 V. When the dissociation energy increased to 60 V, the $[2F_2-2H]^{2-}$ ion completely disappeared while only $[F_2-H]^-$, $[F_2-H-Glc]^-$, $[F_2-H-Glc-Glc]^-$, and glycosyl fragmentation ions were observed in the product ion mass spectra of $[3F_2-2H]^{2-}$. The fragmentation pathways of $[5F_2-2H]^{2-}$ and $[7F_2-2H]^{2-}$ were similar to that of $[3F_2-2H]^{2-}$; hence, only one spectrum of those two anions was selected as an auxiliary example, respectively (Figure 8). The precursor ion $[5F_2-2H]^{2-}$ at *m/z* 1960.24 produced a series of successive losses of F_2 molecules corresponding to $[4F_2-2H]^{2-}$, $[3F_2-2H]^{2-}$, $[2F_2-2H]^{2-}$, $[2F_2-H]^-$, and $[F_2-H]^-$ before losing covalently bonded saccharide moieties (Figure 8a). The product ions $[6F_2-2H]^{2-}$, $[5F_2-2H]^{2-}$, $[4F_2-2H]^{2-}$, $[3F_2-2H]^{2-}$, $[2F_2-2H]^{2-}$, $[2F_2-H]^-$, and $[F_2-H]^-$ were observed in the product ion mass spectra of $[7F_2-2H]^{2-}$ at *m/z* 2744.71 shown in Figure 8b.

Rg3 is one isomer of F_2, containing one sugar chain. The fragmentation pathways of it are clearly distinguishable from that of F_2. The spectra under three collision energies (10, 30, and 50 V) are shown to compare monodesmosidic $[5Rg_3-2H]^{2-}$ and bidesmosidic $[5F_2-2H]^{2-}$ in Figure 9. At 10 V collision energy, both $[3Rg_3-H]^-$ and $[2Rg_3-H]^-$ were observed in the product ion mass spectrum of $[5Rg_3-2H]^{2-}$ at *m/z* 1960.21. The precursor ion $[5Rg_3-2H]^{2-}$ was predominant and $[Rg_3-H]^-$ was absent (Figure 9a). At 30 V collision energy, the daughter ion $[2Rg_3-H]^-$ intensified and $[Rg_3-H]^-$ appeared, while the intensity of $[5Rg_3-2H]^{2-}$ and $[3Rg_3-H]^-$ decreased, as shown in Figure 9b. This indicates that $[Rg_3-H]^-$ can be attributed to dissociation of $[3Rg_3-H]^-$ and/or $[2Rg_3-H]^-$ with increasing energy. As the energy increased to 50 V, $[Rg_3-H]^-$ became the base peak in the mass spectrum. Intensity of $[2Rg_3-H]^-$ reduced approximately onefold compared to 30 V, and $[3Rg_3-H]^-$ completely disappeared (Figure 9c). These results illustrated that $[2Rg_3-H]^-$ and $[3Rg_3-H]^-$ were likely to be

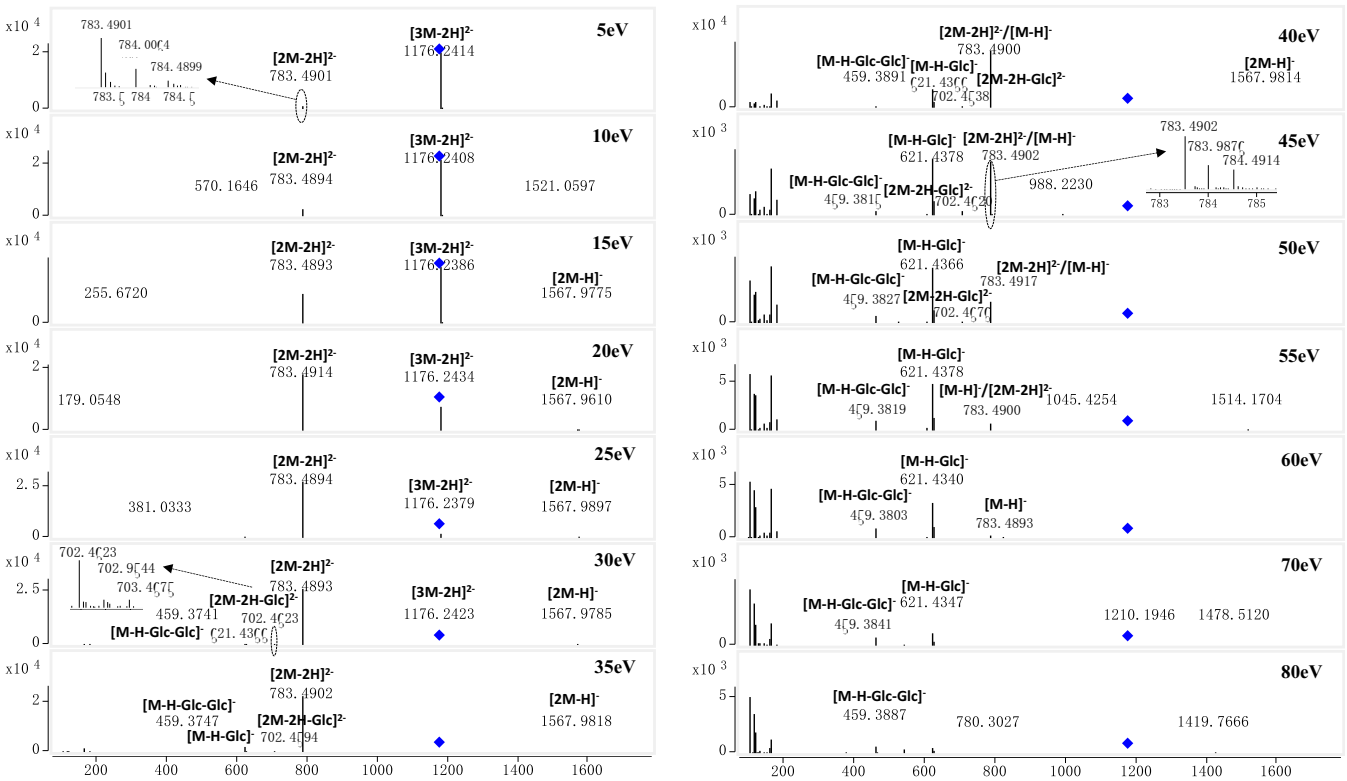

Figure 7. Product ion mass spectra of $[3F_2\text{-}2H]^{2-}$. $[2F_2\text{-}2H]^{2-}$, $[2F_2\text{-}H]^{-}$, and $[F_2\text{-}H]^{-}$ were partly observed in the product ion mass spectra when the CID varied between 5 and 55 eV. When the dissociation energy increased to 60 V, only $[F_2\text{-}H]^{-}$, $[F_2\text{-H-Glc}]^{-}$, $[F_2\text{-H-Glc-Glc}]^{-}$, and glycosyl fragmentation ions were observed in the product ion mass spectra of $[3F_2\text{-}2H]^{2-}$

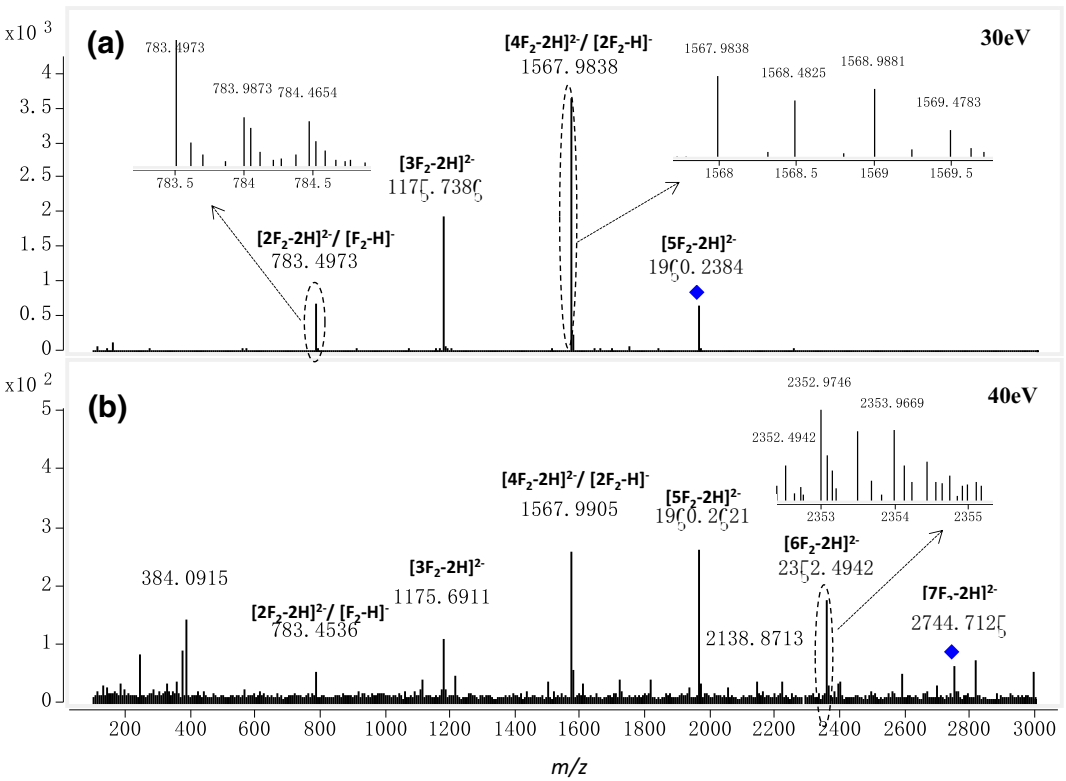

Figure 8. Product ion mass spectra of $[5F_2\text{-}2H]^{2-}$ (**a**) and $[7F_2\text{-}2H]^{2-}$ (**b**). (**a**) Precursor ion $[5F_2\text{-}2H]^{2-}$ at *m/z* 1960.24 produced a series of $[4F_2\text{-}2H]^{2-}$, $[3F_2\text{-}2H]^{2-}$, $[2F_2\text{-}2H]^{2-}$, $[2F_2\text{-}H]^{-}$, and $[F_2\text{-}H]^{-}$. (**b**) Precursor ion $[7F_2\text{-}2H]^{2-}$ at *m/z* 2744.71 produced $[6F_2\text{-}2H]^{2-}$, $[5F_2\text{-}2H]^{2-}$, $[4F_2\text{-}2H]^{2-}$, $[3F_2\text{-}2H]^{2-}$, $[2F_2\text{-}2H]^{2-}$, and $[2F_2\text{-}H]^{-}$

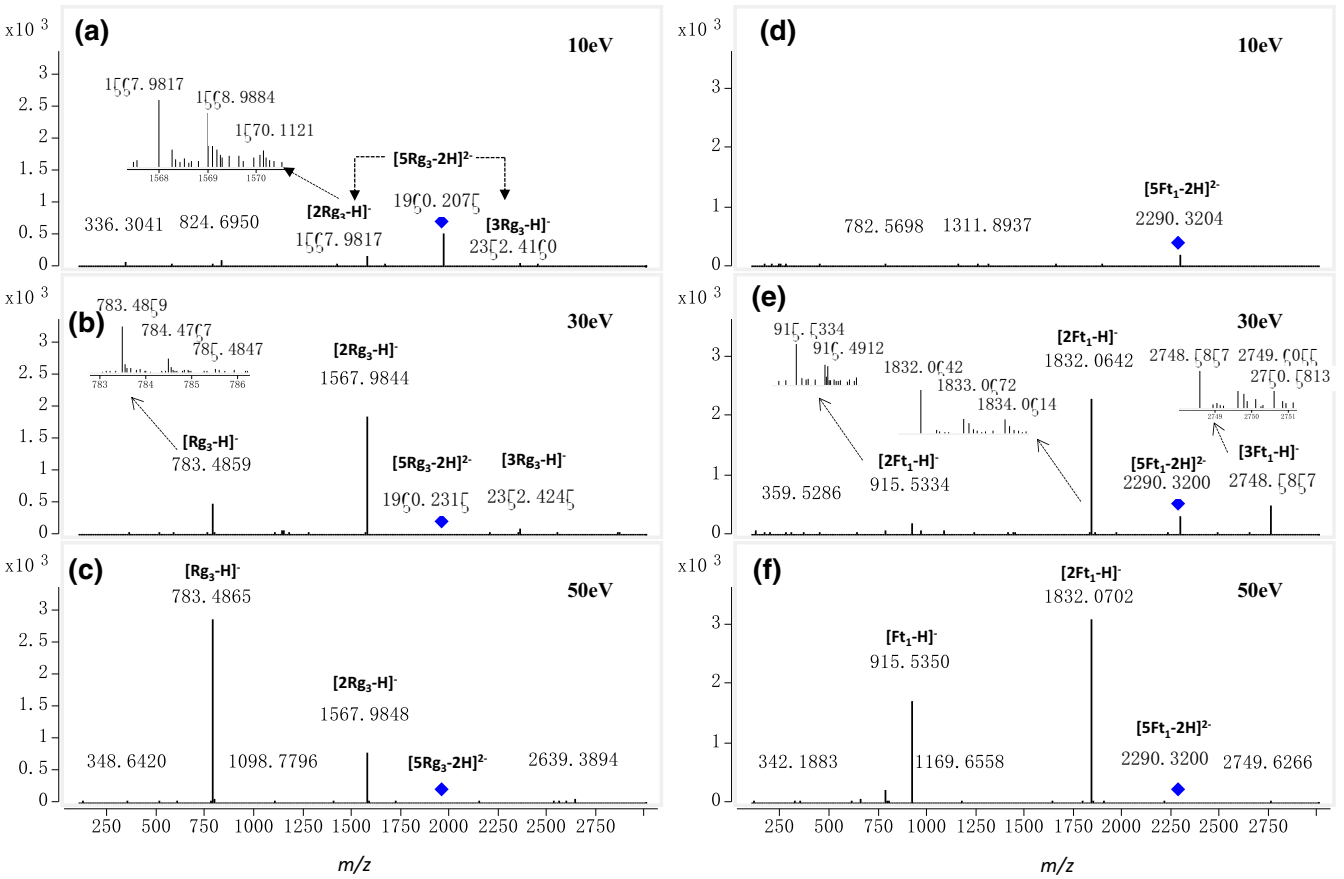

Figure 9. Product ion mass spectra of $[5Rg_3\text{-}2H]^{2-}$ and $[5Ft_1\text{-}2H]^{2-}$. The precursor ion $[5Rg_3\text{-}2H]^{2-}$ at *m/z* 1960.21 was predominant with $[3Rg_3\text{-}H]^-$ and $[2Rg_3\text{-}H]^-$ at a CID of 10 eV (**a**) and $[Rg_3\text{-}H]^-$ also was observed in addition to $[3Rg_3\text{-}H]^-$ and $[2Rg_3\text{-}H]^-$ at a CID of 30 eV (**b**). Similarly, $[3Ft_1\text{-}H]^-$, $[2Ft_1\text{-}H]^-$, and $[Ft_1\text{-}H]^-$ were observed in the product ion mass spectra of $[5Ft_1\text{-}2H]^{2-}$ at *m/z* 2290.32 with a CID of 30 eV (**c**). $[Ft_1\text{-}H]^-$ dramatically increased while $[5Ft_1\text{-}2H]^{2-}$ and $[3Ft_1\text{-}H]^-$ disappeared (**d**)

constituent units of $[5Rg_3\text{-}2H]^{2-}$. Similarly, daughter ions $[3Rg_3\text{-}H]^-$, $[2Rg_3\text{-}H]^-$, and $[Rg_3\text{-}H]^-$ were observed in the product ion mass spectra of $[7Rg_3\text{-}2H]^{2-}$ with collision energies insufficient to cause loss of the sugar group. Since the *m/z* value of $[4Rg_3\text{-}H]^-$ and other singly charged multimer ions with higher degree of polymerization were beyond the *m/z* range, we could not determine whether more polymer ions were involved in the formation of $[7Rg_3\text{-}2H]^{2-}$.

Notoginsenoside Ft_1 is another monodesmosidic ginsenoside and also produced the $[5M\text{-}2H]^{2-}$ anion. When CID was set to 10 V, there was no fragment ion of precursor $[5M\text{-}2H]^{2-}$ as shown in Figure 9d. In addition to the parent ion $[5Ft_1\text{-}2H]^{2-}$, $[3Ft_1\text{-}H]^-$, $[2Ft_1\text{-}H]^-$, and a little $[Ft_1\text{-}H]^-$ were detected in the product ion mass spectrum of $[5Ft_1\text{-}2H]^{2-}$ at *m/z* 2290.32 with CID at 30 V (Figure 9e). In contrast, at 50 V, the product ion $[3Ft_1\text{-}H]^-$ completely disappeared and $[Ft_1\text{-}H]^-$ dramatically increased, which verified that $[M\text{-}H]^-$ was produced by the dissociation of $[3M\text{-}H]^-$ and/or $[2M\text{-}H]^-$ (Figure 9f). Therefore, we propose that $[5M\text{-}2H]^{2-}$ of monodesmosidic ginsenosides is formed when the hydroxyl group of dimer ion ($[2M\text{-}H]^-$) interacts with that of tripolymer ion ($[3M\text{-}H]^-$ through hydrogen bonding during ionization.

In summary, our experimental results demonstrate that $[nM\text{-}2H]^{2-}$ anions are non-covalently bonded multimers based on their concentration-dependent and mass spectrometry cleavage behavior. In addition, ginsenosides containing one sugar and two sugar chains display significantly different aggregation of doubly charged multimer ions anions, which suggests a reasonable explanation for the difference in their formation of $[nM\text{-}2H]^{2-}$. The signal intensity of $[5M\text{-}3H]^{3-}$ and $[7M\text{-}3H]^{3-}$ was too low to conduct the MS/MS experiment. We propose that $[nM\text{-}3H]^{2-}$ anions are non-covalent multimer ions based on concentration-dependent properties. Furthermore, we think multiple deprotonating sites provide the possibility to form so many multicharged anions in the electrospray process. In addition, the two negative charges in multicharged anions are located on separate sugar groups in order to increase degree of charge dispersion to minimize Coulomb repulsion. All in all, formation of these multicharged anions in the electrospray process is quite complex and there may be multiple mechanisms. Both concentration and structure of ginsenosides should affect the formation of multicharged anions.

Conclusions

Numerous multicharged anions eluted simultaneously with ginsenosides from ginseng extract by UPLC-QTOF/MS in

the negative ionization mode. To identify these anions, we chose 14 ginsenoside reference materials (including multiple chemical structures of aglycone and sugar moieties) to study the mass spectrometric behavior of known ginsenosides under the same experimental conditions as analysis of ginseng extract. Compared with previous studies, many doubly and triply charged anions were detected in addition to the common singly charged ions. These included deprotonated quasi-molecular ions, adduct ions, and multimer ions found in the expanded mass range of *m/z* 50–3000. Multicharged ions co-eluting with ginsenosides were formed in the ion source: the diverse ionization behaviors of ginsenosides were responsible for the formation of multiple ions.

We found that all $[nM-2H]^{2-}$ could be formed in the MS of bidesmosidic ginsenosides, whereas higher concentrations of monodesmosidic ginsenosides were required to form $[nM-2H]^{2-}$ anions, in general. $[2M-2H]^{2-}$ and $[3M-2H]^{2-}$ are sensitive to the structural differences of monodesmosidic and bidesmosidic ginsenosides and therefore can be used to differentiate these two types using MS data. Moreover, ginsenosides with sugar moieties attached to the hydroxyl at C-3 form $[nM-2H]^{2-}$ anions more readily than those with sugars at C-6, and ginsenosides with the sugar moiety attached to the hydroxyl at C-20 may not produce the $[nM-2H]^{2-}$ anions. Using $[nM-2H]^{2-}$, three groups of isomeric ginsenosides including (1) Rh_2 and CK; (2) Rg_1, Rf, and F_{11}; and (3) F_2, Rg_2, and Rg_3 could be effectively differentiated. $[M-2H]^{2-}$-type anions were characteristically present on bidesmosidic ginsenosides that have at least three residues. In addition, the chain length of the saccharide moiety appears to be one key factor to the deprotonation of ginsenosides. We have shown that $[nM-2H]^{2-}$ anions are non-covalently bonded multimers from concentration dependence and low-energy CID data. More importantly, the association of $[nM-2H]^{2-}$ was significantly different between monodesmosidic and bidesmosidic ginsenosides.

This study presents a comprehensive understanding of the mass spectrometric behavior of ginsenosides, including the ionization of ginsenosides and association of various anions, allowing for the characterization of unknown ginsenosides and isomers.

Acknowledgements

This work is supported by the Ministry of Science and Technology of the People's Republic of China [2015DFG42460]; Bureau of International Co-operation Chinese Academy of Sciences [121421KYSB20160006]; National Key R&D Program of China [2016YFC1306603]; National Science Foundation [21475128] and Chinese Academy of Science [100Talent Project].

References

1. Yuan, C., Wu, J., Osinski, J.: Ginsenoside variability in American ginseng samples. Am. J. Clin. Nutr. **75**, 600–601 (2002)
2. Wang, Y., Choi, H., Brinckmann, J., Jiang, X., Huang, L.: Chemical analysis of Panax quinquefolius (North American ginseng): a review. J. Chromatogr. A. **1426**, 1–15 (2015)
3. Cheng, Y., Shen, L., Zhang, J.: Anti-amnestic and anti-aging effects of ginsenoside Rg_1 and Rb_1 and its mechanism of action. Acta Pharmacol. Sin. **26**, 143–149 (2005)
4. Mukherjee, P., Maity, N., Nema, N., Sarkar, B.: Bioactive compounds from natural resources against skin aging. Phytomedicine. **19**, 64–73 (2011)
5. Lee, S., Kwon, M., Jang, J., Sohng, J., Jung, H.: The ginsenoside metabolite compound K inhibits growth, migration and stemness of glioblastoma cells. Int. J. Oncol. **51**, 414–424 (2017)
6. Chen, F., Deng, Z., Zhang, B., Xiong, Z., Zheng, S., Tan, H., C., J.: Esterification of ginsenoside Rh_2 enhanced its cellular uptake and antitumor activity in human HepG2 cells. J. Agric. Food Chem. **64**, 253–261 (2016)
7. Wang, B., Cui, J., Liu, A., et al.: Studies on the anti-fatigue effect of the saponins of stems and leaves of Panax ginseng (SSLG). J. Tradit. Chin. Med. **3**, 89–94 (1983)
8. Chen, J., Wu, H., Wang, Q., Yan, C., Liu, K., We, W.: Ginsenoside metabolite compound K suppresses T-cell priming via modulation of dendritic cell trafficking and costimulatory signals, resulting in alleviation of collagen-induced arthritis. J. Pharmacol. Exp. Ther. **353**, 71–79 (2015)
9. Yu, S., Zhou, X., Li, F., Xu, C., Zheng, F., Li, J., Zhao, H., Dai, Y., Liu, S., Feng, Y.: Microbial transformation of ginsenoside Rb_1, Re and Rg_1 and its contribution to the improved anti-inflammatory activity of ginseng. Sci. Rep. **10**, 138–147 (2017)
10. Scholey, A., Ossoukhova, A., Owen, L., Ibarra, A., Pipingas, A., He, K., Roller, M., Stough, C.: Effects of American ginseng (Panax quinquefolius) on neurocognitive function: an acute, randomised, double-blind, placebo-controlled, crossover study. Psychopharmacology. **212**, 345–356 (2010)
11. Qu, D., Yu, H., Liu, Z., Zhang, D., Zhou, Q., Zhang, H., Du, A.: Ginsenoside Rg_1 enhances immune response induced by recombinant Toxoplasma gondii SAG1 antigen. Vet. Parasitol. 179, 28–34 (2011)
12. Dang, D., Shin, E., Kim, D., Tran, H., Jeong, J., Jang, C., Nah, S., Jeong, J., Byun, J., Ko, S., Bing, G., Hong, J., Kim, H.: Ginsenoside re protects methamphetamine-induced dopaminergic neurotoxicity in mice via upregulation of dynorphin-mediated k-opioid receptor and downregulation of substance P-mediated neurokinin 1 receptor. J. Neuroinflammation. **15**, 52–75 (2018)
13. Li, K., Yang, X.: Research progress in the chemical constituents of the stems and leaves of Panax ginseng C. A. Meyer. Mod. Chin. Med. **14**, 47–50 (2012)
14. Qiu, S., Yang, W., Shi, X., Yao, C., Yang, M., Liu, X., Jiang, B., Wu, W., Guo, D.: A green protocol for efficient discovery of novel natural compounds: characterization of new ginsenosides from the stems and leaves of Panax ginseng as a case study. Anal. Chim. Acta. **893**, 65–76 (2015)
15. Georg, S.: Quality valution of ginseng roots. Quantitative HPLC determination of ginsenosides. Dtsch. Apoth. Ztg. **125**, 2052–2055 (1985)
16. Ng, K., Che, C., Wo, S., Tam, P., Lau, A.: Analytical application of acetate anion in negative electrospray ionization mass spectrometry for the analysis of triterpenoid saponins-ginsenosides. Rapid Commun. Mass Spectrom. **20**, 1545–1550 (2006)
17. Wang, H., Zhang, Y., Yang, X., Zhao, D., Wang, Y.: Rapid characterization of ginsenosides in the roots and rhizomes of Panax ginseng by UPLC-DAD-QTOF-MS/MS and simultaneous determination of 19 ginsenosides by HPLC-ESI-MS. J. Ginseng Res. **40**, 382–394 (2016)
18. Li, L., Luo, G., Liang, Q., Hu, P., Wang, Y.: Rapid qualitative and quantitative analyses of Asian ginseng in adulterated American ginseng preparations by UPLC/Q-TOF-MS. J. Pharm. Biomed. Anal. **52**, 66–72 (2010)
19. Park, H., In, G., Kim, J., Cho, B., Han, G., Chang, I.: Metabolomic approach for discrimination of processed ginseng genus (Panax ginseng and *Panax quinquefolius*) using UPLC–QTOF MS. J. Ginseng Res. 38, 59–65 (2014)
20. Sun, B., Xu, M., Li, Z., Wang, Y., Sung, C.: UPLC-Q-TOF-MS/MS analysis for steaming times-dependent profiling of steamed Panax quinquefolius and its ginsenosides transformations induced by repetitious steaming. J. Ginseng Res. **36**, 277 (2012)
21. Mao, Q., Bai, M., Xu, J., Kong, M., Zhu, L., Zhu, H., Wang, Q., Li, S.: Discrimination of leaves of Panax ginseng and P. quinquefolius by ultra-high performance liquid chromatography quadrupole/time-of-flight mass

spectrometry based metabolomics approach. J. Pharm. Biomed. Anal. **97**, 129–140 (2014)
22. Chen, Y., Zhao, Z., Chen, H., Yi, T., Qin, M., Liang, Z.: Chemical differentiation and quality evaluation of commercial Asian and American ginsengs based on a UHPLC-QTOF/MS/MS metabolomics approach. Phytochem. Anal. **26**, 145–160 (2015)
23. Miao, X., Metcalfe, C., Hao, C., March, R.: Electrospray ionization mass spectrometry of ginsenosides. J. Mass Spectrom. **37**, 495–506 (2002)
24. Bai, Y., Gänzle, M.: Conversion of ginsenosides by Lactobacillus plantarum studied by liquid chromatography coupled to quadrupole trap mass spectrometry. Food Res. Int. **76**, 709–718 (2015)
25. Jiang, Y., Cole, R.: Oligosaccharide analysis using anion attachment in negative mode electrospray mass spectrometry. J. Am. Soc. Mass Spectrom. **16**, 60–70 (2005)
26. Kornacki, J., Adamson, J., Håkansson, K.: Electron detachment dissociation of underivatized chloride-adducted oligosaccharides. J. Am. Soc. Mass Spectrom. **23**, 2031–2042 (2012)
27. Wan, D., Yang, H., Yan, C., Song, F., Liu, Z.: Differentiation of glucose-containing disaccharides isomers by fragmentation of the deprotonated non-covalent dimers using negative electrospray ionization tandem mass spectrometry. Talanta. **15**, 870–875 (2013)
28. Ding, J., Anderegg, R.: Specific and nonspecific dimer formation in the electrospray ionization mass spectrometry of oligonucleotides. J. Am. Soc. Mass Spectrom. **6**, 159–164 (1995)
29. Cech, N., Enke, C.: Practical implications of some recent studies in electrospray ionization fundamentals. Mass Spectrom. Rev. **20**, 362–387 (2001)
30. Christensen, L.: Ginsenosides chemistry, biosynthesis, analysis, and potential health effects. Adv Food Nutr Res. **55**, 1–99 (2008)
31. Musende, A., Eberding, A., Wood, C., Adomat, H., Fazli, L., Hurtado-Coll, A., Jia, W., Bally, M., Guns, E.: Pre-clinical valuation of Rh_2 in PC-3 human xenograft model for prostate cancer in vivo: formulation, pharmacokinetics, biodistribution and efficacy. Cancer Chemother Pharmacol. **64**, 1085–1095 (2009)
32. Li, W., Gu, C., Zhang, H., Awang, D., Fitzloff, J., Fong, H., van Breemen, R.: Use of high-performance liquid chromatography-tandem mass spectrometry to distinguish Panax ginseng CA Meyer (Asian ginseng) and Panax quinquefolius L. (North American ginseng). Anal. Chem. **72**, 5417–5422 (2000)